

**THE FE/S RATIO OF PYRRHOTITE GROUP SULFIDES IN CHONDRITES IS RELATED TO THE DEGREE OF OXIDATION.** D. L. Schrader<sup>1</sup>, J. Davidson<sup>1</sup>, T. J. McCoy<sup>2</sup>, T. J. Zega<sup>3</sup>, S. S. Russell<sup>4</sup>, K. J. Domanik<sup>3</sup>, and A. J. King<sup>4</sup>. <sup>1</sup>Center for Meteorite Studies, School of Earth and Space Exploration, Arizona State University, Tempe, AZ 85287-1404, USA (devin.schrader@asu.edu), <sup>2</sup>Dept. of Mineral Sciences, National Museum of Natural History, Smithsonian Institution, Washington, DC USA, <sup>3</sup>Lunar and Planetary Laboratory, University of Arizona, Tucson, Arizona 85721, USA, <sup>4</sup>Department of Earth Sciences, Natural History Museum, Cromwell Road, London, SW7 5BD, UK.

**Introduction:** Fe-sulfides are ubiquitous in chondrites and are sensitive indicators of formation and alteration conditions in the protoplanetary disk and minor Solar System bodies [e.g., 1–12]. The compositions and textures of sulfides can be used to constrain the oxygen and sulfur fugacities, and the histories of aqueous alteration, thermal metamorphism, shock-impact processing, and cooling of the host rock [e.g., 3,5–7,11]. The most abundant sulfides in astromaterials are the pyrrhotite group (ideally  $\text{Fe}_{1-x}\text{S}$  where  $0 \leq x \leq 0.125$ , but  $x$  can be  $\leq 0.2$ ; i.e., FeS [troilite] to  $\text{Fe}_{0.8}\text{S}$ ; e.g., [13]), which can occur with pentlandite,  $(\text{Fe,Ni})_9\text{S}_8$ , and pyrite,  $\text{FeS}_2$  (e.g., [1,5]). The compositions of pyrrhotite in carbonaceous chondrites vary with the degree of aqueous alteration experienced; the at.% Fe/S ratio of pyrrhotite decreases with increasing degrees of aqueous alteration (i.e., Fe/S of pyrrhotite in CI < CM1 < CM2 [1,8,12]). However, troilite (FeS, Fe/S = 1) was observed in aqueously altered and heated CM and CY chondrites [2,4,8].

Here we discuss the Fe/S ratio of pyrrhotite in chondrite groups that cover a wide range of aqueous and thermal histories to evaluate its usefulness as an indicator of parent-body processes and its application to returned samples. Minimally altered samples and those that have experienced varied types/degrees of secondary processing are included because: (1) asteroid Benu is most like CM or CI chondrites [e.g., 14]; (2) asteroid Ryugu is most like heated CI, CM [e.g., 15], or CY chondrites [16]; and (3) both asteroids likely include impact-delivered xenoliths [e.g., 17].

**Samples and Analytical Procedure:** We studied the sulfide compositions of 58 different chondrites; including CI (Alais [Fig. 1], Ivuna, and Orgueil), an ungrouped C1 (MIL 090292), CY (B-7904, Y-82162, Y-86789 [Fig. 2], and Y-980115), CM1/2 (ALH 83100 [Fig. 3] and Kolang) CM2 (Aguas Zarcas, Mighei, and QUE 97990), stage I (A-881458) and stage II (Y-793321) heated CM2s (Nakamura, 2005), CM-like (Sutter's Mill), CO3.00 (DOM 08006), CR1 (GRO 95577), CR-an (Al Rais), CR2 (14 different meteorites), shock-heated CR2 (GRA 06100 and GRO 03116), CV3<sub>OXA</sub> (Allende), CV3<sub>OXB</sub> (Bali), and CV3<sub>Red</sub> (Vigarano), CK4 (ALH 85002 and Karoonda), CK5 (LAR 06868), CK6 (LEW 87009), H3.10 (NWA 3358), L3.05 (QUE 97008), L(LL)3.05 (MET 00452), LL3 (Semarkona and Vicência), LL4 (Hamlet and

Soko-Banja), LL5 (Chelyabinsk and Siena), LL6 (Apley Bridge and Saint-Séverin), R3 (Meteorite Hills [MET] 01149), R3.6 (LaPaz Icefield [LAP] 031275), R5 (LAP 03639), and R6 (LAP 04840 and MIL 11207) chondrites. Some Fe/S ratios were determined from sulfide compositions that we previously published on LL, R, CK, CM, CR2, and CO3 chondrites [5,7,9,10,11,18]. High-resolution images and chemical compositions were obtained with the JEOL-8530F Hyperprobe electron microprobe analyzer (EPMA) at Arizona State University, and the Cameca SX-100 EPMA at the University of Arizona (UA) and at the Natural History Museum (NHM), London, following procedures described in [11].

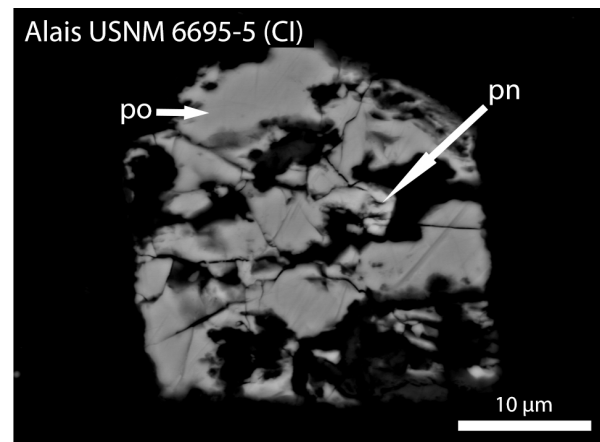


**Figure 1.** BSE image of pyrrhotite (po)-pentlandite (pn) intergrowth in Alais (CI).

**Results:** Pyrrhotite-group sulfides were identified in all samples except the CK4 ALH 85002, CK5, and CK6 chondrites. Pyrite was identified in all CK chondrites. To avoid analyses that could overlap with sub-micron-sized grains of pentlandite, we define Ni-poor pyrrhotite as containing less than 1 wt.% Ni [11]; these analyses were used to determine the at.% Fe/S ratios. The pyrrhotite-group sulfide troilite (Fe/S  $\approx$  1) was found in the H3.10, L3.05, all LL chondrites, the CO3.00, all CV3s, the CYs, the CR1, all CR2s, some CM2s, the CM-like chondrite Sutter's Mill, and the R3 chondrite. Fe-depleted pyrrhotite ( $\text{Fe}_{1-x}\text{S}$ ; Fe/S from  $<1$  to 0.8) was found in the CIs (Fig. 1), CYs (Fig. 2), the C1-ung, the CR-an Al Rais, some sulfides within CR2

chondrites, the CM1/2s (e.g., Fig. 3), the CM2s, the CM-like Sutter's Mill, some sulfides in LL chondrites, one sulfide in the H3.10, the R3 to R6 chondrites, and a single grain in the CK4 Karoonda. No troilite was found in the CK chondrites and only a single grain of pyrrhotite was found in the CK4 Karoonda, which has the lowest Fe/S ratio analyzed here.

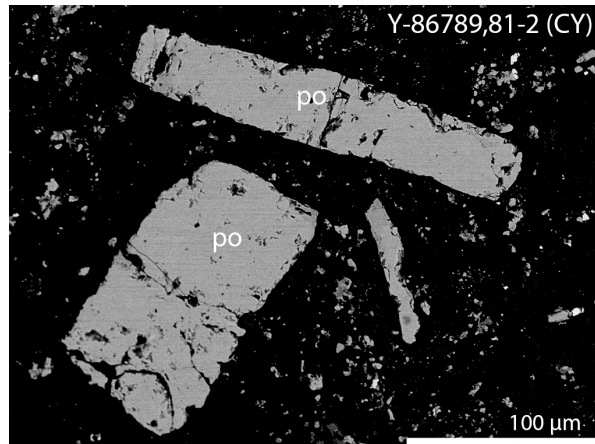


**Figure 2.** BSE of pyrrhotite (po) laths in Y-86789 (CY).

**Discussion:** The average Fe/S ratio of pyrrhotite varies among meteorite groups and petrographic types within meteorite groups. The trend in average Fe/S ratio of all chondrites studied appears complicated, the order from lowest to highest average Fe/S ratio separated by petrographic type is: CK4 < CI < R6 < CM1/2 ≤ CR-an < C1-ung ≤ R5 ≤ R3.6 ≤ R3 ≤ CM2 ≤ CV3<sub>OxA</sub> ≈ CR1 ≈ CR2 ≈ CY ≈ LL4 ≤ L3.05 ≤ LL5 ≤ LL3 ≈ CV3<sub>OxB</sub> ≤ H3.10 ≈ LL6 ≤ CV3<sub>Red</sub> ≤ L(LL)3.05 ≈ CO3.00. The average Fe/S ratio of pyrrhotite generally trends with the degree of aqueous alteration in unheated carbonaceous chondrites. It is likely that internal sample heterogeneities, thermal and aqueous alteration, and differences in sulfur and oxygen fugacities (e.g., the CK4 and R chondrites) all contribute to the order of Fe/S ratios. For example, as previously noted [2,8], troilite is present in aqueously and thermally altered carbonaceous chondrites (e.g., the CYs studied here). Therefore, using the at.% Fe/S ratio of pyrrhotite as a universal proxy for the degree of aqueous or thermal alteration is not warranted.

Comparing the average Fe/S ratio to the degree of oxidation of each meteorite [e.g., 19], we find a relationship between the average Fe/S ratio and the bulk meteorite oxidation state. The most reduced chondrites contain troilite and the most oxidized (via thermal or aqueous alteration) chondrites contain Fe-depleted pyrrhotite. The presence of troilite or Fe-depleted pyrrhotite in a chondrite is an indicator of the relative oxygen fugacity of its formation or alteration. This rela-

tionship is the case whether the sample is unaltered, aqueously altered, and/or thermally metamorphosed, as oxidation can occur in the protoplanetary disk or in the parent body during aqueous or thermal alteration.

**Summary:** While there are trends with the at.% Fe/S ratio of pyrrhotite with thermal and aqueous alteration in some meteorite groups, there is a universal trend with the Fe/S ratio with degree of oxidation. This finding has important implications for the analysis of sulfides in chondrites and returned samples.

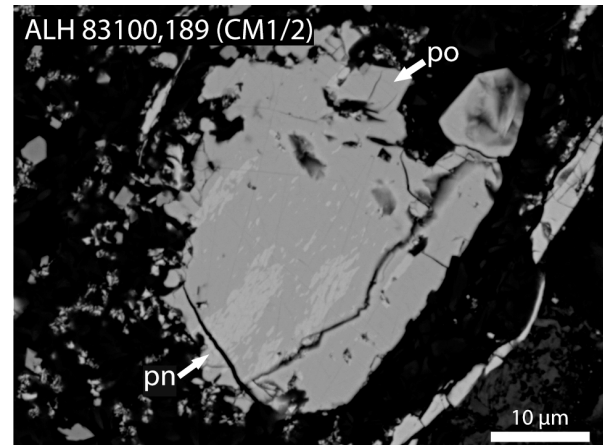


**Figure 3.** BSE image of pyrrhotite (po)-pentlandite (pn) intergrowth in ALH 83100 (CM1/2).

**References:** [1] Bullock E. S. et al. (2005) *GCA*, 69, 2687–2700. [2] Nakamura T. (2005) *J. Mineral. Petrol. Sci.*, 100, 260–272. [3] Kimura M. et al. (2011) *M&PS*, 46, 431–442. [4] Harries D. and Langenhorst F. (2013) *M&PS*, 48, 879–903. [5] Schrader D. L. et al. (2016) *GCA*, 189, 359–376. [6] Harries D. and Zolensky M. E. (2016) *M&PS*, 51, 1096–1109. [7] Schrader D. L. et al. (2018) *EPSL*, 504, 30–37. [8] Harries D. (2018) *2018 Hayabusa Symposium* (abstract). [9] Davidson J. et al. (2019a), *GCA*, 267, 240–256. [10] Davidson J. et al. (2019b), *GCA*, 265, 259–278. [11] Schrader D. L. and Zega T. J. (2019), *GCA*, 264, 165–179. [12] Kimura M. et al. (2020), *Polar Science*, 26, 100565. [13] Haldar S. K. (2017), In *Platinum-Nickel-Chromium Deposits*, 1–35. [14] Hamilton V. E. et al. (2019) *Nat. Astron.*, 3, 332–340. [15] Kitazato K. et al. (2019) *Science*, 364, 272–275. [16] King A. J. et al. (2019) *Geochem.*, 79, 125531. [17] DellaGiustina et al (2020) *Nat. Astron.* <https://doi.org/10.1038/s41550-020-1195-z>. [18] Schrader D. L. et al. (2015) *M&PS*, 50, 15–50. [19] Righter K. et al. (2006) In *Meteorites and the Early Solar System II*. pp. 803–828.

**Acknowledgements:** We thank the NiPR, Smithsonian Institution, NASA, NSF, ASU, NHM, and I/P for the samples used in this study, and NASA grant NNX17AE53G (DLS PI, TJZ Co-I) for funding this research.